

SwarnRaft: Leveraging Consensus for Robust Drone Swarm Coordination in GNSS-Degraded Environments

Kapel Dev, Yash Madhwal, *Member, IEEE* Sofia Shevelo, Pavel Osinenko, Yury Yanovich, *Member, IEEE*

Abstract—Unmanned aerial vehicle (UAV) swarms are increasingly used in critical applications such as aerial mapping, environmental monitoring, and autonomous delivery. However, the reliability of these systems is highly dependent on uninterrupted access to the Global Navigation Satellite Systems (GNSS) signals, which can be disrupted in real-world scenarios due to interference, environmental conditions, or adversarial attacks, causing disorientation, collision risks, and mission failure. This paper proposes SwarnRaft, a blockchain-inspired positioning and consensus framework for maintaining coordination and data integrity in UAV swarms operating under GNSS-denied conditions. SwarnRaft leverages the Raft consensus algorithm to enable distributed drones (nodes) to agree on state updates such as location and heading, even in the absence of GNSS signals for one or more nodes. In our prototype, each node uses GNSS and local sensing, and communicates over WiFi in a simulated swarm. Upon signal loss, consensus is used to reconstruct or verify the position of the failed node based on its last known state and trajectory. Our system demonstrates robustness in maintaining swarm coherence and fault tolerance through a lightweight, scalable communication model. This work offers a practical and secure foundation for decentralized drone operation in unpredictable environments.

Index Terms—Blockchain, UAV swarms, Raft consensus, GNSS-denied environments, Fault tolerance

I. INTRODUCTION

Rapid proliferation of autonomous swarms, including unmanned aerial vehicles (UAVs), ground robots, and maritime systems, has enabled transformative applications in domains such as logistics, infrastructure monitoring, agriculture, and disaster response [1, 2, 3]. These distributed systems rely heavily on precise coordination, predominantly facilitated by *Global Navigation Satellite Systems* (GNSS) such as **GPS**, **GLONASS**, **Galileo**, and **BeiDou** [4]. However, GNSS signals are often unreliable in real-world conditions, such as urban canyons, dense vegetation, or indoor and subterranean environments. To mitigate these limitations, systems frequently integrate *Inertial Navigation Systems* (INS) to improve robustness and continuity.

As swarm deployments scale in size and mission complexity, achieving reliable consensus among agents becomes a critical challenge, one that draws direct parallels to problems in distributed computing and blockchain technologies. In this context, swarms must maintain accurate and synchronized state information (e.g., position, velocity, heading) despite partial failures and environmental interference [5, 6].

Several mission-critical scenarios exemplify the need for robust consensus mechanisms. In urban package delivery, GNSS reflections from buildings can compromise altitude coordination, and a single altimeter failure can lead to collisions [7]. During bridge inspections, complete GNSS denial requires drones to maintain spatial awareness solely through local sensing and swarm coordination. Agricultural spray missions present additional complexities, as drones must adjust for dynamic weight changes during chemical dispersion in rural settings, often degraded by GNSS.

These operational constraints echo classic challenges of distributed systems, yet swarm robotics introduces distinct requirements [8, 9]. Unlike traditional consensus algorithms that emphasize Byzantine fault tolerance, such as those used in permissioned or permissionless blockchain systems, swarm consensus must prioritize low-latency agreement, operate under stringent resource constraints, and address crash-fault-dominated failure models [10, 11, 12]. The core principles of consensus remain: ensuring *termination* (all non-faulty agents reach a decision), *agreement* (consistency across decisions), and *integrity* (decisions are based on valid inputs), even in the presence of partial system failures [13].

UAV swarms operate under unique constraints, including limited compute and energy resources, intermittent connectivity, and bounded-delay communication networks. Consequently, traditional blockchain consensus protocols such as Proof-of-Work and Proof-of-Stake are ill-suited due to their computational and energy overhead [14, 15]. Similarly, Byzantine Fault-Tolerant (BFT) protocols, e.g., PBFT, Tendermint, Exonum [16, 17, 18], assume adversarial behavior and incur unnecessary complexity for typical crash-fault scenarios in swarms. This creates a compelling opportunity to adapt crash-tolerant consensus protocols, such as *Raft* [19], which are designed for environments where nodes (the drones) may fail by crashing, but not by acting maliciously. Raft's lightweight leader-based architecture is well suited to the resource-constrained and real-time nature of swarm robotics.

To address these challenges, we propose **SwarnRaft**, a *consensus-driven* positioning and *crash-tolerant* system designed for drone swarms. Our approach leverages the Raft consensus algorithm to enable drones to communicate and synchronize over a distributed network, even in partially GNSS-denied environments. SwarnRaft integrates GNSS and INS data to enable drones to exchange critical state information such as position and heading. In the event of GNSS loss or sensor malfunction, the swarm uses consensus to reconstruct

or verify the location and trajectory of affected nodes based on shared data and prior motion. This consensus-driven estimation ensures that the swarm remains cohesive and continues its mission safely, even when individual drones experience degraded sensing.

Our work makes the following key contributions:

- **Adaptation of Raft for Swarm Environments:** We adapt the Raft consensus protocol to support real-time coordination in UAV swarms, prioritizing low-latency decision-making and resilience under crash-fault conditions typical in GNSS-compromised settings.
- **Sensor Fusion for Robust State Estimation:** SwarmRaft combines GNSS and INS data using a distributed consensus framework to produce robust, fault-tolerant state estimates. This fusion mitigates the effects of signal intermittency, spoofing, and sensor drift, enhancing the swarm's overall situational awareness and operational reliability.
- **Empirical Validation in Realistic Scenarios:** We evaluate SwarmRaft through a comprehensive set of experiments and simulations, demonstrating its effectiveness in preserving swarm cohesion and operational continuity across urban and natural terrains.

This work bridges the fields of swarm robotics and distributed consensus, advancing resilience in GNSS-degraded environments. SwarmRaft builds on established consensus algorithms, demonstrating their applicability to UAV swarm coordination. Our approach maintains theoretical rigor while prioritizing practical deployability, showing significant improvements in both simulated and real-world scenarios.

II. RELATED WORK

Decentralized coordination mechanisms for UAV swarms have gained increasing attention, particularly through consensus-based and blockchain-backed approaches. While leader-follower architectures have shown success in formation control [20], their reliance on central nodes introduces vulnerabilities to single points of failure. In contrast, distributed strategies offer greater resilience. Tariverdi et al. [21] present a formation control framework tailored to UAV dynamics, and Jia et al. [22] demonstrate decentralized estimation and coordination in quadcopter swarms.

In the context of Industrial IoT, Seo et al. [23] propose a co-design framework that jointly optimizes communication scheduling and consensus execution to meet strict latency requirements. Although their setting involves fixed infrastructure, their insights into delay-aware consensus coordination are applicable to mobile multi-agent systems. Similarly, Ilić et al. [24] introduce adaptive asynchronous gossip algorithms for heterogeneous sensor networks, offering resilience and scalability through weighted message exchange without requiring global synchronization. While their work focuses on distributed estimation in sensor-rich environments, the underlying principles of asynchronous fault-tolerant consensus motivate swarm-scale extensions.

Blockchain-based protocols add guarantees of trust and tamper resistance in decentralized coordination. P-Raft [25]

optimizes consensus in consortium settings, and DTPBFT [26] dynamically adjusts trust levels in UAV networks. Yazdinejad et al. [27] propose a zone-based drone authentication framework using a Delegated Proof-of-Stake (DDPOS) mechanism to enable secure, low-latency inter-zone handovers in smart city deployments.

Comparative analyses of consensus algorithms such as Raft, PBFT, and PoW have focused on trade-offs in scalability, fault tolerance, and energy use [28, 29, 30, 31]. Surveys such as [32] highlight the challenges of adapting these mechanisms to real-time robotics, particularly under energy and processing constraints.

Research on fault-tolerant swarm behavior includes predictive failure mitigation [33], self-healing topologies [34], and GNSS spoofing resilience [35]. Robust navigation under sensor failures [36] and adaptive topology control [37] further emphasize the need for distributed, resilient solutions.

Real-world deployments, such as outdoor flocking and coordinated flight demonstrations [38], underline the feasibility of translating algorithmic designs to physical swarm systems.

Despite these advances, many existing frameworks either impose significant communication or computational overhead, or fail to address the specific fault models and coordination challenges faced by UAV swarms operating under GNSS degradation and adversarial interference. In contrast, **SwarmRaft** introduces a lightweight, crash-tolerant localization framework that combines peer-based voting with distributed fault recovery, offering robust performance in dynamic and partially compromised environments.

III. PROPOSED SOLUTION

A. Overview of the Consensus Scheme

In modern UAV swarms, individual GNSS or INS readings alone cannot guarantee resilience against sensor faults or deliberate spoofing. Our consensus scheme, **SwarmRaft**, leverages peer-to-peer distance measurements, crash fault-tolerant communication consensus, and a Byzantine-resilient evaluation mechanism to detect and correct malicious or *faulty* position reports. At each time step k , the swarm determines the position of each UAV (node). To determine the positions, nodes communicate via Raft consensus and elect a leader for the step. The leader collects every node's raw GNSS and INS fused position, tests if it is consistent with others, recovers it if required, and returns the results to the nodes.

This design achieves fault tolerance under the assumption that up to f nodes' sensors may be corrupted, so long as $n \geq 2f + 1$, where n is the total number of nodes in the swarm. *Honest* nodes never collude to mislead, and initial positions are trusted. The result is a distributed protocol that detects spoofing and significant sensor drift, locally filters out unreliable data, and recovers accurate positions through consensus based on neighbor estimates. Communication cost remains $O(n)$ for the leader and $O(1)$ for other nodes.

A high-level workflow of **SwarmRaft** in the case of a determined leader at a single step k is as follows:

- 1) **Sense:** Each UAV measures GNSS and INS.

- 2) **Inform**: Raw fused position is sent to the leader (as a client's transaction).
- 3) **Estimate**: The leader recomputes each UAV's position from range constraints.
- 4) **Evaluate**: The leader determines if the data of each sensor is *faulty* or *honest* based on residuals.
- 5) **Recover**: If a sensor is determined to be *faulty*, the leader replaces its data with the median of peer estimates.
- 6) **Finalize**: The leader sends the final results to all nodes.

B. System & Threat Model

Each UAV in our scheme is modeled as a fully-capable sensing and communication node. At each discrete time step k , node i collects an absolute position measurement $\mathbf{z}_{i,k}^{\text{GNSS}}$ from its onboard GNSS receiver; because GNSS alone can drift or be spoofed, the UAV also carries an INS that produces short-term motion increments $\Delta \mathbf{u}_{i,k}$ through accelerometers and gyroscopes. To bind these two modalities and detect inconsistent readings, every UAV is further equipped with a ranging sensor (for example, ultra-wideband or RSSI-based) that yields noisy inter-node distances $d_{ij,k}$ to each neighbor j . Finally, nodes share all measurements and voting messages over an authenticated broadcast channel protected by pre-distributed cryptographic keys, so that neither message forgery nor tampering can occur undetected.

We assume the communication graph among the n UAVs is fully connected and synchronous: in each protocol round every node can exchange messages with every other node, and timing is sufficiently well aligned that messages from step k are received before step $k+1$ begins. This idealization lets us focus on sensor faults rather than network delays or partitions. To tolerate up to f arbitrarily *faulty* or malicious sensors, we require the bound $n \geq 2f+1$. Under this constraint, even if f nodes report completely corrupted GNSS or ranging data (or collude to bias their votes), the remaining *honest* nodes still form a majority that can detect and override any bad information.

Assumption 1: Nodes' compute and communication modules are *honest*, authorized, and synchronous.

Assumption 2: Only GNSS sensors can be Byzantine, while INS are reliable. Up to f nodes' GNSS sensors out of n may be arbitrarily corrupted, where $n \geq 2f+1$.

Assumption 3: True positions at time $k=0$ are securely known.

We model three classes of adversarial behavior against which our consensus scheme must defend:

Attack scenario 1 (GNSS Spoofing Attack): An adversary corrupts the satellite positioning signals received by up to f UAVs, causing each compromised node to report position measurements $\mathbf{z}_{i,k}^{\text{GNSS}}$ that are offset by an arbitrary, potentially time-varying bias. Such spoofing can be orchestrated remotely and may remain undetected by the individual UAV's receiver.

However, our inter-node consistency checks and consensus mechanism aim to reveal any GNSS readings that deviate significantly from the peer-estimated location.

Attack scenario 2 (Ranging-Tampering Scenario): The adversary injects errors into the inter-UAV distance measurements $d_{ij,k}$. This could be accomplished by jamming or forging ultra-wideband pulses (or manipulating RSSI readings), causing one or more *honest* nodes to compute incorrect range constraints.

Since our fused position estimates rely on the integrity of these distance measurements, the protocol's voting and median-based recovery step are designed to mitigate the impact of up to f such corrupted range reports.

Attack scenario 3 (Collusion Among Faulty Sensors): We allow for collusion among up to f *faulty* sensors across different UAVs. In this worst-case scenario, compromised nodes coordinate both their reported measurements and their votes in the **SwarmRaft** protocol in an attempt to sway the swarm's decision about a particular node's status.

By enforcing the requirement $n \geq 2f+1$ and using majority thresholds, the scheme guarantees that *honest* votes outnumber colluding malicious votes, ensuring that no coalition of size $\leq f$ can force an incorrect global decision.

C. Position Estimation

At each time step $k \in \mathbb{N}$, the UAV with index $i \in \{1, \dots, n\}$ obtains two complementary measurements of its state. First, the GNSS receiver produces a direct but noisy readout of the true position $\mathbf{x}_{i,k}$:

$$\mathbf{z}_{i,k}^{\text{GNSS}} = \mathbf{x}_{i,k} + \mathbf{v}_{i,k}^{\text{GNSS}}, \quad \mathbf{v}_{i,k}^{\text{GNSS}} \sim \mathcal{N}(0, R_{\text{GNSS}}),$$

where R_{GNSS} is the GNSS measurement covariance, and $\mathcal{N}(m, \sigma^2)$ is a normal distribution with mathematical expectation m and variance σ^2 . Second, the INS dead-reckons from the previous time step by integrating acceleration and rotation increments $\Delta \mathbf{u}_{i,k}$, yielding

$$\mathbf{x}_{i,k}^{\text{INS}} = \mathbf{x}_{i,k-1} + \Delta \mathbf{u}_{i,k} + \mathbf{v}_{i,k}^{\text{INS}}, \quad \mathbf{v}_{i,k}^{\text{INS}} \sim \mathcal{N}(0, R_{\text{INS}}).$$

Thus, the INS provides high-rate relative motion at the cost of accumulating drift, while GNSS provides drift-free absolute position with higher instantaneous noise.

To cross-check these two sensor streams, each UAV also measures its distance to every other UAV. If UAV j measures the range to UAV i , the reading satisfies

$$d_{ij,k} = \|\mathbf{x}_{i,k} - \mathbf{x}_{j,k}\| + \eta_{ij,k}, \quad \eta_{ij,k} \sim \mathcal{N}(0, \sigma_d^2).$$

This geometric constraint links the true positions of nodes i and j and can reveal inconsistencies when one node's GNSS or INS has been spoofed or drifted excessively.

D. Fused Estimate at Peer j for Node i

Peer j combines the raw GNSS reading from i with a range-based estimate to form a minimum-variance fusion. Denote the range-only estimate as

$$\mathbf{x}_{i,k}^{\text{range},(j)} = \mathbf{x}_{j,k}^{\text{INS}} + \frac{d_{ij,k}}{\|\mathbf{x}_{j,k}^{\text{INS}} - \mathbf{x}_{i,k-1}\|} (\mathbf{x}_{i,k-1} - \mathbf{x}_{j,k}^{\text{INS}}).$$

A linear fusion of the two estimates,

$$\hat{\mathbf{x}}_{i,k}^{(j)} = \alpha \mathbf{z}_{i,k}^{\text{GNSS}} + (1 - \alpha) \mathbf{x}_{i,k}^{\text{range},(j)},$$

achieves minimum mean-square error when the weight α equals the ratio of the range-estimate variance to the total variance. Specifically, if σ_{GNSS}^2 and σ_{range}^2 denote the variances of the GNSS and range-based estimates (obtainable from R_{GNSS} and linearization of the range constraint), then

$$\alpha = \frac{\sigma_{\text{range}}^2}{\sigma_{\text{GNSS}}^2 + \sigma_{\text{range}}^2}, \quad 1 - \alpha = \frac{\sigma_{\text{GNSS}}^2}{\sigma_{\text{GNSS}}^2 + \sigma_{\text{range}}^2}.$$

With this choice, the fused estimate $\hat{\mathbf{x}}_{i,k}^{(j)}$ has variance equal to the harmonic sum of the individual variances, ensuring optimal use of both GNSS and inter-UAV ranging information.

E. Fault Detection

In this phase, the leader scrutinizes the consistency of a reported position by comparing the fused estimate against the original GNSS reading. A large discrepancy indicates that either the reporting node's sensors or the peer's range measurement may be *faulty*. To make this precise, we define a residual, apply a statistically-justified threshold, and then cast a binary vote.

The leader measures the consistency of node's i report with the data from node j based on the received positions $\mathbf{z}_{i,k}$ and $\mathbf{z}_{j,k}$, it first computes its own fused estimate $\hat{\mathbf{x}}_{i,k}^{(j)}$ as described earlier. The *residual*

$$e_{i,k}^{(j)} = \|\hat{\mathbf{x}}_{i,k}^{(j)} - \mathbf{z}_{i,k}\|.$$

measures the Euclidean distance between the peer's estimate and the raw GNSS reading. Under nominal (non-attacked) conditions, this residual is driven by zero-mean sensor noise from both GNSS and ranging, so it remains small with high probability.

To decide whether $e_{i,k}^{(j)}$ is abnormally large, we set a threshold

$$T = \mu_e + 3\sigma_e,$$

where μ_e and σ_e are the mean and standard deviation of the residual under *honest*-sensor operation (obtainable by offline calibration). By the Gaussian tail bound, the probability that an *honest* residual exceeds T is at most

$$P(e_{i,k}^{(j)} > T) \leq \exp(-\frac{9}{2}) < 0.01.$$

Thus any $e_{i,k}^{(j)} > T$ is strong evidence of a sensor fault or spoofing.

1) *Local Vote Broadcast*: Based on the threshold test, peer j issues a binary vote

$$v_{i,k}^{(j)} = \begin{cases} +1, & e_{i,k}^{(j)} \leq T, \\ -1, & e_{i,k}^{(j)} > T. \end{cases}$$

A vote of +1 indicates *honest*, while -1 signals *faulty*. This local decision is then broadcast to all other peers, forming the input for the subsequent **SwarmRaft** stage.

Leader computes votes for each node and flags their GNSS as *honest* or *faulty*, i.e., compute $S_i = \sum_j v_{i,k}^{(j)}$:

- If $S_i \geq n - f$, decide i is *honest*.
- If $S_i < -(n - f)$, decide i is *faulty*.

F. Position Correction & Recovery

If decision i is *faulty*, the position is set to

$$\tilde{\mathbf{x}}_{i,k} = \text{median}_j \{\hat{\mathbf{x}}_{i,k}^{(j)}\}.$$

Node i resets its INS state to $\tilde{\mathbf{x}}_{i,k}$; otherwise it retains its fused estimate.

Note: With a low probability we can flag one or several *honest* sensors as *faulty*, which may lead to a majority of the sensors flagged as *faulty* for the current k . In such a case, we do not compute the median during the recovery phase, but recover based on INS only.

G. Security & Fault-Tolerance Analysis

The security and fault-tolerance guarantees of **SwarmRaft** arise from its algorithmic design, the assumptions of the threat model, and the underlying Raft consensus protocol.

Safety: SwarmRaft ensures safety through majority voting by enforcing the condition $n \geq 2f + 1$, the system guarantees that *honest* nodes always outnumber any coalition of up to f *faulty* or malicious nodes. This majority threshold prevents incorrect decisions from being adopted, even in the presence of adversarial behavior.

Liveness: In a synchronous network setting, the protocol guarantees liveness as long as a majority of nodes remain honest and responsive. The Raft algorithm enables reliable leader election and, once a leader is in place, timely progress is maintained throughout the swarm through efficient rounds of position estimation, fault detection, and recovery.

Integrity: All inter-node communications are authenticated using pre-distributed cryptographic keys, preventing forgery and tampering. Consensus-based validation ensures the trustworthiness of the reported data. Although rare statistical anomalies can incorrectly flag an *honest* sensor as *faulty*, such false positives are mitigated by majority voting. In edge cases where too many nodes are flagged, the system falls back to inertial (INS) data for continuity, preserving mission integrity at the cost of reduced accuracy.

Communication Efficiency: SwarmRaft is designed to scale efficiently. The leader incurs a communication and computation cost of $O(n)$ per round, while non-leader nodes communicate only with the leader at $O(1)$ cost. This model minimizes bandwidth usage and processing load as the swarm scales. Raft log replication further ensures consistency across all nodes.

Fault Tolerance: The protocol tolerates up to f Byzantine faults, including GNSS spoofing, range manipulation and collusion. By requiring $n \geq 2f + 1$, SwarmRaft ensures that honest node votes dominate and that consensus decisions remain trustworthy even under adversarial conditions. The coordination of the leader of the Raft and the replicated logs reinforce fault-tolerant behavior during ongoing operations.

Recovery: When faults are detected, SwarmRaft employs a robust median-based recovery strategy that replaces outlier or corrupted readings with consensus estimates derived from peer data. This allows the swarm to maintain stable formation and control even under localized sensor failures. Recovery decisions are consistently propagated via Raft's replication mechanism, preserving swarm-wide state alignment.

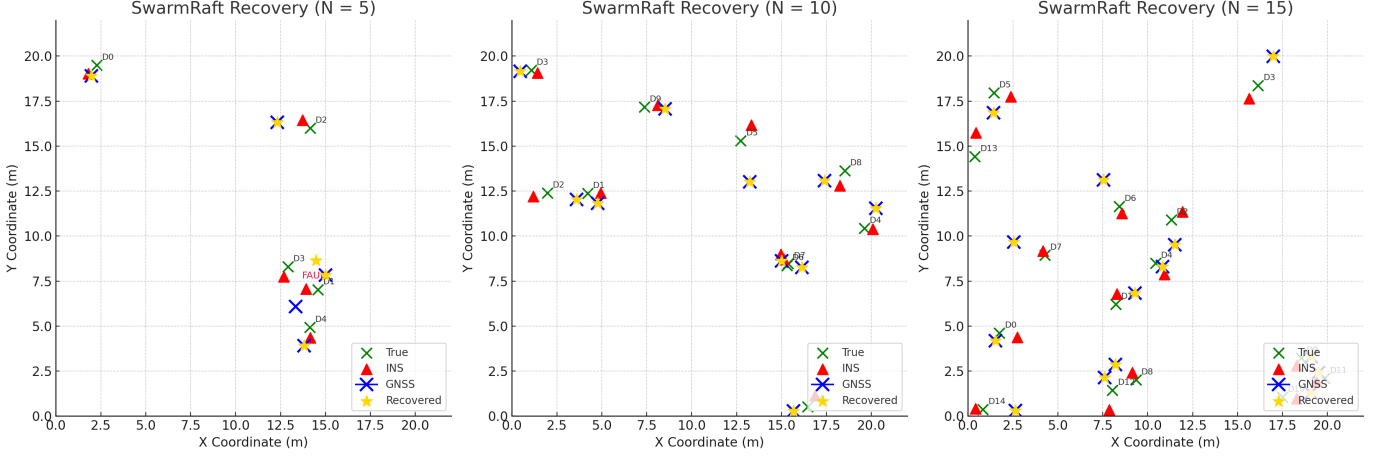


Fig. 1: Visualization of SwarmRaft recovery under different swarm sizes ($N = 5, 10, 15$). Yellow stars represent recovered positions using consensus and range-based fusion.

IV. PROTOTYPE IMPLEMENTATION

To evaluate SwarmRaft under adversarial localization scenarios, we developed a modular simulation framework in Python that models both the dynamics and vulnerabilities of drone swarms. The framework simulates each drone's ground-truth motion, inertial navigation estimates, GNSS observations (including spoofed signals), and noisy inter-drone ranging data. A dedicated leader node module performs fused position estimation, fault detection through residual analysis and majority voting, and robust recovery based on peer consensus. To support performance benchmarking, the simulator includes tools for running large-scale Monte Carlo experiments that vary swarm size and attacker configuration, producing statistical metrics including MAE. Additionally, the framework supports real-time visualization and post-simulation plotting to analyze error evolution and swarm behavior.

Each drone instance maintains a ground-truth position vector $\mathbf{x}_i^{\text{true}}$, a GNSS-based measurement \mathbf{z}_i , and an inertial estimate $\mathbf{x}_i^{\text{INS}}$ defined by:

$$\mathbf{x}_i^{\text{INS}} = \mathbf{x}_i^{\text{prev}} + \Delta \mathbf{u}_i + \varepsilon_{\text{INS}}, \quad \mathbf{z}_i = \mathbf{x}_i^{\text{true}} + \varepsilon_{\text{GNSS}}. \quad (1)$$

Inter-agent fusion is performed via weighted averaging of local and remote estimates. The fused position from agent j to agent i is given by:

$$\hat{\mathbf{x}}_i^{(j)} = \alpha \mathbf{z}_i + (1 - \alpha) \left(\mathbf{x}_j^{\text{INS}} + \frac{d_{ij} \cdot (\mathbf{x}_i^{\text{prev}} - \mathbf{x}_j^{\text{INS}})}{\|\mathbf{x}_i^{\text{prev}} - \mathbf{x}_j^{\text{INS}}\|} \right). \quad (2)$$

The weighting coefficient α depends on the variance of GNSS and range measurements:

$$\alpha = \frac{\sigma_r^2}{\sigma_r^2 + \sigma_z^2}. \quad (3)$$

Each agent compares the fused estimate $\hat{\mathbf{x}}_i^{(j)}$ to its own GNSS reading. If the residual is below a threshold τ , a positive vote is cast; otherwise, the vote is negative:

$$v_{ij} = \begin{cases} +1, & \text{if } \|\hat{\mathbf{x}}_i^{(j)} - \mathbf{z}_i\| \leq \tau \\ -1, & \text{otherwise} \end{cases}. \quad (4)$$

Faulty agents are identified when the number of negative votes exceeds the trust threshold $(n - f)$, where n is the swarm size and f is the maximum number of faults considered. Position recovery is performed by aggregating fused estimates from peers using the coordinate-wise median:

$$\hat{\mathbf{x}}_i = \text{median} \left\{ \hat{\mathbf{x}}_i^{(j)} \mid j \in \mathcal{N}(i) \right\}. \quad (5)$$

The prototype accommodates configurable attack injection, including GNSS spoofing, range distortion, and randomized attacker behavior. The implementation serves as the experimental foundation for the visual and quantitative evaluations discussed in subsequent sections. The source code for *SwarmRaft* is publicly available on GitHub [39].

V. NUMERICAL EXPERIMENTS

A. Qualitative Results for Position Recovery

Figure 1 illustrates the SwarmRaft consensus-based recovery mechanism across varying swarm sizes $N \in \{5, 10, 15\}$, simulating aerial drone localization using GNSS and INS. Each subfigure demonstrates how noisy or spoofed measurements are corrected through distributed voting and recovery. This visualization not only showcases concrete recovery behavior but also reveals the spatial structure of localization errors in both small- and large-scale swarms, complementing the accompanying statistical evaluation.

Each drone D_i is annotated with:

- **Green circle (o):** the ground-truth position $\mathbf{x}_i^{\text{true}}$.
- **Blue cross (x):** the GNSS measurement $\mathbf{z}_i = \mathbf{x}_i^{\text{true}} + \varepsilon_i^{\text{GNSS}}$, where $\varepsilon_i^{\text{GNSS}} \sim \mathcal{N}(0, \sigma^2 \mathbf{I})$.
- **Red triangle (Δ):** the INS estimate $\mathbf{x}_i^{\text{INS}}$, which accumulates integration errors and noise.
- **Yellow star (★):** the recovered position $\hat{\mathbf{x}}_i$ computed via the SwarmRaft algorithm.

The SwarmRaft protocol fuses inter-drone distance measurements and local INS readings using a consensus scheme. Each node receives fused position suggestions from its neighbors and performs majority voting to detect inconsistencies. If a node is suspected to be compromised, its position is recovered via a robust aggregation (e.g., coordinate-wise median) of neighbor estimates.

Mathematically, the fused estimate from a neighbor j to a node i is computed as:

$$\hat{\mathbf{x}}_i^{(j)} = \alpha \mathbf{z}_i + (1 - \alpha) \left(\mathbf{x}_j^{\text{INS}} + \frac{d_{ji} \cdot (\mathbf{x}_i^{\text{prev}} - \mathbf{x}_j^{\text{INS}})}{\|\mathbf{x}_i^{\text{prev}} - \mathbf{x}_j^{\text{INS}}\|} \right). \quad (6)$$

Here, $\alpha = \frac{\sigma_r^2}{\sigma_r^2 + \sigma_{\text{GNSS}}^2}$ is a weighting coefficient derived from error variances, and d_{ji} is the noisy range measurement between drones j and i .

Consensus voting is performed by comparing fused estimates to local GNSS readings. If the residual is above a threshold τ , the vote is negative. A node is considered faulty if it receives more than $(n - f)$ negative votes, where f is the assumed maximum number of compromised nodes.

B. Quantitative Evaluation Across Swarm Sizes and Attacks

To complement the visual analysis of SwarmRaft's behavior, we conduct a large-scale statistical evaluation using simulated drone swarms with varying sizes and attack conditions. For each swarm size $N \in \{5, 10, 15\}$ and each number of attacked drones $f \in \{1, 2, \dots, N - 1\}$, we run 10 Monte Carlo trials. During each trial, f drones are randomly selected to be compromised via GNSS spoofing and range manipulation. The remaining drones follow the nominal sensing model, where the GNSS and INS errors are drawn from zero-mean Gaussian distributions.

Each Monte Carlo trial produces two sets of localization error metrics:

- **GNSS Baseline Error:** The mean absolute error (MAE) is calculated based on the raw GNSS readings:

$$\text{MAE}_{\text{GNSS}} = \frac{1}{N} \sum_{i=1}^N \|\mathbf{z}_i - \mathbf{x}_i^{\text{true}}\|.$$

- **SwarmRaft-Recovered Error:** The same metrics are computed using the recovered positions $\hat{\mathbf{x}}_i$ after consensus-based correction:

$$\text{MAE}_{\text{SwarmRaft}} = \frac{1}{N} \sum_{i=1}^N \|\hat{\mathbf{x}}_i - \mathbf{x}_i^{\text{true}}\|.$$

The results are aggregated across all trials and shown in Figure 2. Each curve depicts the average error as a function of the number of attacked drones f , grouped by the total swarm size N .

We observe that:

- 1) GNSS-only estimates degrade significantly as f increases, particularly in larger swarms.
- 2) The SwarmRaft algorithm consistently reduces MAE compared to raw GNSS readings, even when a majority of drones are attacked.

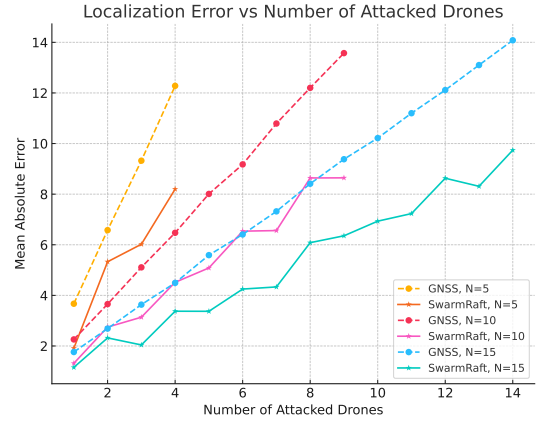


Fig. 2: Error trends for GNSS and SwarmRaft-recovered positions under varying attack intensities and swarm sizes. Each curve is averaged over 10 trials.

- 3) The recovered errors remain stable as swarm size increases, suggesting scalability and resilience of the consensus mechanism.

These results demonstrate that SwarmRaft is capable of robust fault detection and position recovery even under adversarial and large-scale conditions.

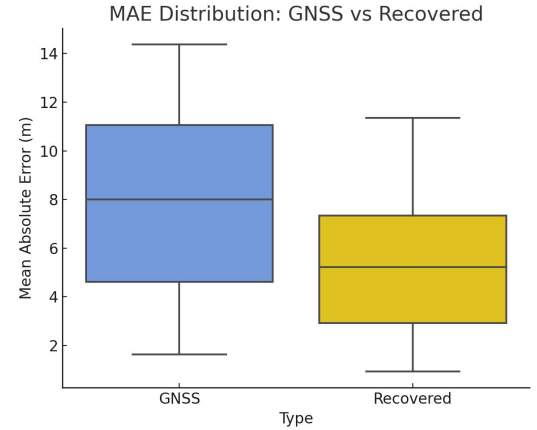


Fig. 3: Boxplot of mean absolute error (MAE) for GNSS-only positioning and SwarmRaft-recovered estimates across all simulation trials. The recovered positions exhibit lower median error and reduced variance, indicating improved accuracy and robustness under adversarial conditions.

Figure 3 compares the distribution of localization errors under GNSS-only and SwarmRaft-recovered positioning across diverse simulation trials. The GNSS error distribution shows a higher median, wider spread, and more extreme values, reflecting its vulnerability to spoofing and sensor faults. In contrast, the SwarmRaft-corrected estimates demonstrate a substantially reduced median error and tighter interquartile range, with fewer outliers. This indicates both improved accuracy and robustness, underscoring the protocol's effectiveness in mitigating adversarial localization noise through consensus and peer fusion.

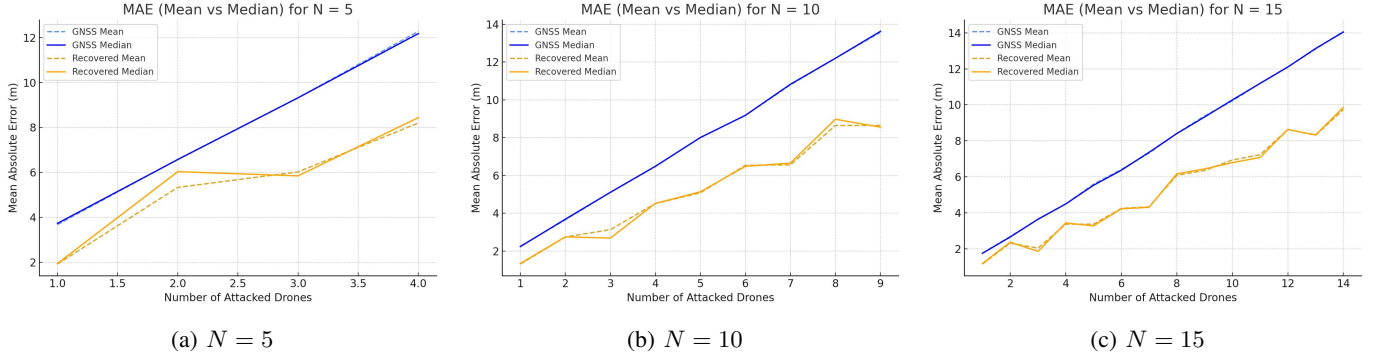


Fig. 4: Comparison of mean and median absolute localization errors for GNSS and SwarmRaft-recovered estimates under varying numbers of attacked drones. Each subfigure corresponds to a different swarm size. Dashed lines represent means; solid lines denote medians. SwarmRaft reduces sensitivity to outliers, especially in larger swarms.

C. Comparison of Mean and Median Errors

Figures 4 present the evolution of absolute localization errors as the number of compromised agents increases, across swarm sizes $N = 5, 10$, and 15 . Each subplot compares GNSS-only positioning with estimates recovered using the SwarmRaft protocol.

GNSS results exhibit a growing discrepancy between mean and median errors as more nodes are spoofed, revealing vulnerability to extreme outliers. In contrast, the SwarmRaft-based estimates maintain a smaller gap between these statistics, indicating robustness to adversarial noise. This behavior suggests that the consensus and fusion mechanism is capable of filtering out anomalous contributions even in highly degraded conditions. Additionally, as the swarm size increases, the recovered medians become increasingly stable, reflecting the benefits of larger peer sets in collaborative state estimation.

VI. DISCUSSION

The experiments in Section V evaluate the practical behavior and performance of the proposed SwarmRaft protocol under controlled adversarial conditions, including GNSS spoofing and range measurement perturbations. Simulations were performed in varying swarm sizes and numbers of compromised nodes.

Figure 1 visually demonstrates SwarmRaft’s ability to detect and isolate faulty agents, even in small swarms with limited redundancy. The recovered positions align closely with the truth of the ground, highlighting the effectiveness of peer triangulation and consistency-based voting. The quantitative results in Figures 3 and 4 demonstrate that SwarmRaft significantly reduces both mean and median localization errors, with accuracy improving as the size of the swarm increases. As more peers become available, the system maintains low median errors even in the presence of multiple compromised nodes. The corresponding boxplot further confirms the robustness of the method, showing reduced variance and fewer outliers under adversarial conditions.

These findings highlight the core strengths of SwarmRaft, including its robustness to localized spoofing without requiring prior attacker identification, its scalability in decentralized deployments with varying trust levels, and its adaptability to

sensor noise and signal degradation. The protocol operates without a centralized fusion authority and tolerates Byzantine behavior under mild density assumptions, making it well-suited for distributed robotic swarms operating in partially adversarial environments.

Nonetheless, several limitations remain. The current design assumes bounded noise and reliable relative ranging, which may degrade in GNSS-denied urban canyons or under active jamming. The protocol also treats all peers equally, without incorporating trust weighting or historical behavior. Moreover, while efficient in simulation, real-time deployment may face latency and packet loss challenges that affect performance.

VII. CONCLUSION

This paper presented SwarmRaft, a consensus-based protocol for resilient UAV swarm localization in GNSS-degraded and adversarial environments. By fusing inertial measurements with peer-to-peer ranging and validating positional consistency through distributed voting, SwarmRaft achieves accurate state estimation even in the presence of GNSS spoofing and range manipulation. In contrast to centralized or purely sensor-driven approaches, it integrates fault detection, consensus-based validation, and position recovery into a lightweight and scalable framework inspired by Raft.

Extensive simulations across varying swarm sizes and attack conditions demonstrated that SwarmRaft consistently reduces both mean and median localization errors relative to raw GNSS measurements. Notably, the protocol maintains stable performance even as the number of compromised agents increases, with larger swarms enhancing robustness through increased redundancy and more reliable peer estimates.

Beyond adversarial fault mitigation, SwarmRaft offers a generalizable architecture for collaborative localization under uncertainty, requiring minimal assumptions about trust, infrastructure, or communication hierarchy. Its compatibility with standard UAV sensing modalities (GNSS, INS, and ranging) and its ability to operate in fully decentralized settings support its applicability in real-world missions such as disaster response, infrastructure inspection, and autonomous logistics.

Future work will focus on extending the protocol with dynamic trust modeling, adaptive voting thresholds, and

confidence-weighted fusion to enhance resilience against sensor drift and coordinated adversarial behavior. In addition, performance under asynchronous communication and packet loss should be evaluated, alongside validation on physical UAV swarms operating in real-world conditions. Ultimately, SwarmRaft establishes a principled foundation for robust, autonomous multi-agent systems capable of reliable operation in contested and degraded environments.

ACKNOWLEDGMENT

We acknowledge the use of ChatGPT and DeepSeek in enhancing the readability and clarity of this manuscript. These tools were employed to assist in refining language and improving the overall presentation of the content. However, the authors retain full responsibility for the integrity, accuracy, and intellectual contributions of the research at all stages.

REFERENCES

- [1] A. A. Laghari, A. K. Jumani, R. A. Laghari, and H. Nawaz, “Unmanned aerial vehicles: A review,” *Cognitive Robotics*, vol. 3, pp. 8–22, 2023.
- [2] M. AlMarshoud, M. S. Kiraz, and A. H. Al-Bayatti, “Security, privacy, and decentralized trust management in vanets: A review of current research and future directions,” *ACM Computing Surveys*, vol. 56, pp. 1–39, 10 2024.
- [3] I. Bae and J. Hong, “Survey on the developments of unmanned marine vehicles: Intelligence and cooperation,” *Sensors*, vol. 23, p. 4643, 5 2023.
- [4] B. Bhatta, *Global Navigation Satellite Systems*, 2nd ed. CRC Press, 2021.
- [5] M.-T. O. Hoang, K. A. R. Grøntved, N. van Berkel, M. B. Skov, A. L. Christensen, and T. Merritt, *Drone Swarms to Support Search and Rescue Operations: Opportunities and Challenges*, 2023, pp. 163–176.
- [6] N. M. Elfatih, E. S. Ali, and R. A. Saeed, *Navigation and Trajectory Planning Techniques for Unmanned Aerial Vehicles Swarm*, 2023, pp. 369–404.
- [7] K. Kuru, D. Ansell, W. Khan, and H. Yetgin, “Analysis and optimization of unmanned aerial vehicle swarms in logistics: An intelligent delivery platform,” *IEEE Access*, vol. 7, pp. 15 804–15 831, 2019.
- [8] S. Bano, A. Sonnino, M. Al-Bassam, S. Azouvi, P. McCorry, S. Meiklejohn, and G. Danezis, “Sok: Consensus in the age of blockchains,” in *Proceedings of the 1st ACM Conference on Advances in Financial Technologies*. ACM, 10 2019, pp. 183–198.
- [9] M. Raikwar, N. Polyanskii, and S. Müller, “Sok: Dag-based consensus protocols,” in *2024 IEEE International Conference on Blockchain and Cryptocurrency (ICBC)*. IEEE, 2024, pp. 1–18. [Online]. Available: <https://ieeexplore.ieee.org/document/10634358/>
- [10] V. Buterin, “On public and private blockchains - ethereum blog,” 2015. [Online]. Available: <https://blog.ethereum.org/2015/08/07/on-public-and-private-blockchains/>
- [11] B. Group and J. Garzik, “Public versus private blockchains. part 1: Permissioned blockchains,” *bitfury.com*, pp. 1–23, 2015. [Online]. Available: <http://bitfury.com/content/5-white-papers-research/public-vs-private-pt1-1.pdf>
- [12] —, “Public versus private blockchains part 2: Permissionless blockchains,” *bitfury.com*, pp. 1–20, 2015. [Online]. Available: <http://bitfury.com/content/5-white-papers-research/public-vs-private-pt2-1.pdf>
- [13] C. Dwork, N. Lynch, and L. Stockmeyer, “Consensus in the presence of partial synchrony,” *Journal of the ACM*, vol. 35, pp. 288–323, 4 1988. [Online]. Available: <http://portal.acm.org/citation.cfm?doid=42282.42283>
- [14] S. Nakamoto, “Bitcoin: A peer-to-peer electronic cash system,” *www.bitcoin.org*, pp. 1–9, 2008. [Online]. Available: <https://bitcoin.org/bitcoin.pdf>
- [15] A. Kiayias, A. Russell, B. David, and R. Oliynykov, *Ouroboros: A Provably Secure Proof-of-Stake Blockchain Protocol*. Springer, Cham, 8 2017, vol. 10401 LNCS, pp. 357–388. [Online]. Available: http://link.springer.com/10.1007/978-3-319-63688-7_12
- [16] M. Castro and B. Liskov, “Practical byzantine fault tolerance,” *Proceedings of the Third Symposium on Operating Systems Design OSDI ’99*, pp. 173–186, 1999. [Online]. Available: <http://pmg.csail.mit.edu/papers/osdi99.pdf>
- [17] J. Kwon, “Tendermint : Consensus without mining,” pp. 1–10, 2014. [Online]. Available: tendermint.com/docs/tendermint.pdf
- [18] Y. Yanovich, I. Ivashchenko, A. Ostrovsky, A. Shevchenko, and A. Sidorov, “Exonum: Byzantine fault tolerant protocol for blockchains,” *bitfury.com*, pp. 1–36, 2018. [Online]. Available: <https://bitfury.com/content/downloads/wp-consensus-181227.pdf>
- [19] D. Ongaro and J. Ousterhout, “In search of an understandable consensus algorithm,” in *Proceedings of the 2014 USENIX Annual Technical Conference, USENIX ATC 2014*, 2014.
- [20] R. Rafifandi, D. L. Asri, E. Ekawati, and E. M. Budi, “Leader-follower formation control of two quadrotor uavs,” *SN Applied Sciences*, vol. 1, pp. 1–12, 2019.
- [21] A. Tariverdi and J. Torresen, “Rafting towards consensus: Formation control of distributed dynamical systems,” 2023. [Online]. Available: <https://arxiv.org/abs/2308.10097>
- [22] Z. Jia, M. Hamer, and R. D’Andrea, “Distributed estimation, control and coordination of quadcopter swarm robots,” *arXiv preprint arXiv:2102.07107*, 2021.
- [23] H. Seo, J. Park, M. Bennis, and W. Choi, “Communication and consensus co-design for distributed, low-latency, and reliable wireless systems,” *IEEE Internet of Things Journal*, vol. 8, pp. 129–143, 1 2021.
- [24] N. Ilić, M. Vučetić, A. Makarov, R. Petrović, and M. Punt, “Adaptive asynchronous gossip algorithms for consensus in heterogeneous sensor networks,” *IEEE Internet of Things Journal*, vol. 12, pp. 25 516–25 532, 7 2025.
- [25] S. Lu, X. Zhang, R. Zhao, L. Chen, J. Li, and G. Yang, “P-raft: an efficient and robust consensus mechanism for consortium blockchains,” *Electronics*, vol. 12, no. 10, p. 2271, 2023.
- [26] P. Han, X. Wu, and A. Sui, “Dtpbft: A dynamic and highly trusted blockchain consensus algorithm for uav swarm,” *Computer Networks*, vol. 250, p. 110602, 2024.
- [27] A. Yazdinejad, R. M. Parizi, A. Dehghantanha, H. Karimipour, G. Srivastava, and M. Aledhari, “Enabling drones in the internet of things with decentralized blockchain-based security,” *IEEE Internet of Things Journal*, vol. 8, pp. 6406–6415, 4 2021.
- [28] V. Sharma and N. Lal, “A novel comparison of consensus algorithms in blockchain,” *Advances and Applications in Mathematical Sciences*, vol. 20, no. 1, pp. 1–13, 2020.
- [29] “Hyperledger fabric: a distributed operating system for permissioned blockchains,” in *Proceedings of the Thirteenth EuroSys Conference*. ACM, 4 2018, pp. 1–15. [Online]. Available: <https://dl.acm.org/doi/10.1145/3190508.3190538>
- [30] P. Kostyuk, S. Kudryashov, Y. Madhwal, I. Maslov, V. Tkachenko, and Y. Yanovich, “Blockchain-based solution to prevent plastic pipes fraud,” in *2020 Seventh International Conference on Software Defined Systems (SDS)*. IEEE, 4 2020, pp. 208–213. [Online]. Available: <https://ieeexplore.ieee.org/document/9143879/>
- [31] B. Borzdov, M. Minchenok, and Y. Yanovich, “Practical vulnerabilities in byzantine fault-tolerant blockchain consensus protocols,” in *2023 XVIII International Symposium Problems of Redundancy in Information and Control Systems (REDUNDANCY)*. IEEE, 10 2023, pp. 94–99.
- [32] U. S. Aditya, R. Singh, P. K. Singh, and A. Kalla, “A survey on blockchain in robotics: Issues, opportunities, challenges and future directions,” *Journal of Network and Computer Applications*, vol. 196, p. 103245, 2021.
- [33] J. O’Keefe and A. G. Millard, “Predictive fault tolerance for autonomous robot swarms,” *arXiv preprint arXiv:2309.09309*, 2023.
- [34] V. S. Varadharajan, D. St-Onge, B. Adams, and G. Beltrame, “Swarm relays: Distributed self-healing ground-and-air connectivity chains,” *IEEE Robotics and Automation Letters*, vol. 5, no. 4, pp. 5347–5354, 2020.
- [35] A. RANGANATHAN, A. BELFKI, and P. CLOSAS, “The impact of gnss spoofing on unmanned aerial vehicle swarms,”
- [36] J. Hu, H. Niu, J. Carrasco, B. Lennox, and F. Arvin, “Fault-tolerant cooperative navigation of networked uav swarms for forest fire monitoring,” *Aerospace Science and Technology*, vol. 123, p. 107494, 2022.
- [37] G. Wang, H. Luo, X. Hu, H. Ma, and S. Yang, “Fault-tolerant communication topology management based on minimum cost arborescence for leader-follower uav formation under communication faults,” *International Journal of Advanced Robotic Systems*, vol. 14, no. 2, p. 1729881417693965, 2017.
- [38] G. Vászrhelyi, C. Virág, G. Somorjai, N. Tarcai, T. Szörényi, T. Nepusz, and T. Vicsek, “Outdoor flocking and formation flight with autonomous aerial robots,” in *2014 IEEE/RSJ International Conference on Intelligent Robots and Systems*. IEEE, 2014, pp. 3866–3873.
- [39] Y. Madhwal, “Swarmraft,” <https://github.com/yashmadhwal/SwarmRaft>, 2025, gitHub repository.